ORIGINAL ARTICLE

Transport and Optical Properties of *n*-Butylamine + Alkanols (C₃–C₄) Mixtures for Enhanced CO₂ Absorption

Sweety Verma[1,6] · Suman Gahlyan[2] · Payal Bhagat[3] · Manju Rani[4] · Seetu Rana[5] · Yongjin Lee[1] ⃝ · Sanjeev Maken[6]

Abstract

Reducing carbon emissions has emerged as a critical challenge, and among various methods, solvent-based CO_2 capture technology is the most widely employed. Amines, particularly effective solvents for CO_2 capture, play a significant role in this process. To advance this technology, it is essential to understand the thermodynamic properties of the interactions between the constituent components. In this study, we examined the deviation in dynamic viscosity ($\Delta\eta$), and the deviation in refractive index (Δn_D) calculated from the measured η and n_D data for *n*-butylamine (NBA) with alkanol systems. The temperature range for our study was 298.15–318.15 K. We utilized the Ab-initio approach for $\Delta\eta$ data analysis. Our findings revealed that the depolymerization power of alkanol is dependent on the unlike interactions. Furthermore, we employed various correlations/mixing rules to predict the η as well as n_D values from the experimental pure components data. The standard deviation was utilized to express the predictive abilities of these correlations.

Keywords Dynamic viscosity · *n*-Butyl amine · Alkanol · Refractive index · Ab-initio approach · CO_2 absorption

✉ Yongjin Lee
    yongjin.lee@inha.ac.kr

✉ Sanjeev Maken
    sanjeevmakin@gmail.com

1   Department of Chemistry and Chemical Engineering, Education and Research Center for Smart Energy and Materials, Inha University, Yonghyeon Campus, Incheon 22212, Republic of Korea

2   Department of Applied Sciences and Humanities, Panipat Institute of Engineering and Technology, Samalkha 132102, India

3   Department of Chemistry, Deenbandhu Chhotu Ram University of Science and Technology, Murthal 131039, India

4   Department of Chemical Engineering, Deenbandhu Chhotu Ram University of Science and Technology, Murthal 131039, India

5   Department of Mathematics, Government College, Hisar 125001, India

6   Department of Chemistry, Netaji Subhas University of Technology, New Delhi 110078, India

Introduction

There has been a growing emphasis on developing technologies that effectively capture and store CO_2 emissions from various sources [1–4]. The scientific community and policymakers worldwide are increasingly concerned about the rise in global temperatures due to escalating CO_2 [5, 6]. As a result, the development of efficient technologies for capturing and storing CO_2 emitted from diverse sources has gained momentum. The fundamental concept of CCS involves capturing CO_2 from industrial processes, transporting it to storage sites, and safely storing it underground [7, 8]. However, significant technical, economic, and environmental challenges hinder the development and deployment of CCS technologies [9].

The CO_2 capture system is a critical component of CCS technologies, which entails isolating CO_2 from flue gas streams emitted by industrial facilities or power plants. Solvent-based CO_2 capture technologies have attracted significant interest due to their high efficiency in capturing CO_2 and relatively low cost [10, 11]. Alkylamines are a class of organic compounds containing both amine and alcohol functional groups [12, 13]. They are widely used as solvents for CO_2 capture, due to their high reactivity with CO_2 and ability to form stable CO_2-alkylamine complexes [14, 15].

n-Butylamine is one of the most effective alkylamines for CO_2 capture, as it has a high CO_2 absorption capacity and low energy requirement for solvent regeneration [16]. The capacity of amines and alcohols to form hydrogen bonds leads to the association of these components, and alcohol is chosen as the other component to enhance amine solubility.

To accurately interpret intermolecular interactions between the components, it is crucial to thoroughly understand their thermodynamic properties [17, 18]. This study examines the dynamic viscosity (η) and refractive index (n_D) of n-butylamine (NBA) with alkanol at 0.1 MPa pressure and temperatures ranging from 298.15 to 318.15 K. The deviation in viscosity ($\Delta\eta$) was calculated using the measured viscosity data. Additionally, an *Ab-initio* approach was employed to analyze the $\Delta\eta$ data. The $\Delta\eta$ data were analyzed using multiple correlations. The refractive index (n_D) reflects the speed of light, which is influenced by the medium density and specific interactions between binary mixture molecules [19, 20]. An increase in refractive index corresponds to a denser medium, resulting in slower light speed. By analyzing the n_D data, we investigate the intermolecular behavior in *n*-butylamine (NBA) + alkanol mixtures at temperatures between 298.15 and 318.15 K. The $\Delta\eta$ and Δn_D data were fitted using the Redlich–Kister (RK) equation, and the Δn_D for these systems, based on pure component data, were evaluated using various mixing rules.

Table 1 Details of chemical source, purity (mass fraction) and analysis method

Chemical name	CAS number	Source	Initial purity (%) (by vendor)	Final purity (%) (GC analysis)
NBA	109–73–9	Sigma	0.995	0.996
n-propanol	71–23–8	Sigma	≥ 0.995	0.996
sec-propanol	67–63–0	Sigma	≥ 0.995	0.996
n-butanol	71–36–3	Sigma	≥ 0.994	0.996
sec-butanol	78–92–2	Merck	0.995	0.997
iso-butanol	78–83–1	Sigma	≥ 0.990	0.994

Experimental Section

Materials

NBA and alkanol were obtained from Sigma-Aldrich and Merck. Before use, they were stored in amber-colored bottles over molecular sieves (3 Å) (Sigma-Aldrich) for 72 h [21]. Table 1 presents the specification and CAS numbers of the chemicals, along with purity reported by the vendors and by analysis performed using gas chromatography. The purities of the compounds were verified by comparing the measured ρ, η and n_D data with literature values, as shown in Table 2.

Methods

The ρ, η and n_D data of the pure components and binary mixtures were measured by using a vibrating tube densimeter (DSA-5000, Anton Paar), a rolling-ball viscometer (LOVIS 2000 ME, Anton Paar) integrated with a densimeter, and a refractometer (Abbemat-200, Anton Paar) as presented in Table 3. The temperature has a precision of ± 0.01 K. The instrument was calibrated every day at 298.15 K using ultra-pure water and cleaned with warm water and ethanol after every sample [37–40]. Binary mixtures were prepared using an analytical balance (OHAUS, AR224CN) with a precision of ± 0.1 mg. The measurement uncertainties were 5×10^{-4} g cm^{-3} for ρ, 0.003 mPa s for η, 0.0001 for mole fraction, and 0.0005 for n_D [19].

Results and Discussion

Viscosity

Utilizing Eq. (1), the $\Delta\eta$ values were computed from the measured η data of pure components and mixtures. The $\Delta\eta$ of binary mixtures are shown in Fig. 1 and Table 3.

Table 2 Densities (ρ/g cm^{-3}), viscosity (η/mPa s) and refractive index (n_D) of the pure compound at the temperature 298.15 K and pressure 0.1 MPa

Compound	ρ/g cm^{-3}		η/mPa s		n_D	
	This work	Literature	This work	Literature	This work	Literature
NBA	0.73996	0.7390 [22]	0.576	0.578 [23] 0.4689 [24]	1.3988	1.3987 [25]
n-propanol	0.79998	0.7996 [26]	1.981	1.981 [27]	1.3832	1.3832 [28]
sec-propanol	0.78130	0.78128 [29]	2.069	2.070 [30]	1.3751	1.3752 [31]
n-butanol	0.80581	0.80575 [32]	2.560	2.560 [33]	1.3967	1.3967 [28]
sec-butanol	0.80273	0.8026 [22]	3.067	3.068 [33]	1.3951	1.3951 [34]
iso-butanol	0.79812	0.79816 [35]	3.411	3.410 [33]	1.3939	1.3939 [36]

Standard uncertainties *u*: *u* (T) = 0.01 K; u(p) = 0.04 MPa; u(ρ) = 5×10^{-4} g cm^{-3}; u(η) = 0.003 mPa s; u(n_D) = 0.0005; (level of confidence = 95%, k = 2).

Table 3 Experimental viscosity (η/mPa s), deviation in viscosity ($\Delta\eta$/mPa s), refractive index (n_D) and deviation in refractive index (Δn_D) for NBA (1) + alkanol (2) mixtures

x_1	η	$\Delta\eta$	n_D	Δn_D	η	$\Delta\eta$	n_D	Δn_D	η	$\Delta\eta$	n_D	Δn_D
$T=298.15$ K					$T=303.15$ K				$T=308.15$ K			
NBA (1) + *n*-propanol (2)												
0.0797	1.780	−0.087	1.3857	0.0013	1.579	−0.067	1.3833	0.0008	1.415	−0.044	1.3812	0.0007
0.1649	1.603	−0.141	1.3875	0.0017	1.416	−0.125	1.3852	0.0014	1.282	−0.086	1.3831	0.0011
0.2522	1.427	−0.192	1.3891	0.0020	1.263	−0.170	1.3869	0.0017	1.158	−0.117	1.3849	0.0014
0.3457	1.254	−0.231	1.3907	0.0021	1.118	−0.199	1.3886	0.0019	1.035	−0.140	1.3867	0.0016
0.4374	1.098	−0.255	1.3922	0.0022	0.995	−0.209	1.3901	0.0019	0.923	−0.154	1.3884	0.0017
0.5359	0.960	−0.252	1.3936	0.0020	0.881	−0.202	1.3916	0.0018	0.814	−0.158	1.3901	0.0017
0.6415	0.832	−0.228	1.3951	0.0019	0.776	−0.176	1.3930	0.0015	0.710	−0.149	1.3917	0.0014
0.7509	0.730	−0.174	1.3965	0.0016	0.682	−0.135	1.3944	0.0012	0.619	−0.123	1.3933	0.0011
0.8682	0.636	−0.099	1.3976	0.0009	0.592	−0.081	1.3958	0.0007	0.542	−0.075	1.3949	0.0007
0.9339	0.589	−0.052	1.3982	0.0004	0.548	−0.044	1.3965	0.0004	0.507	−0.040	1.3957	0.0004
$T=313.15$ K									$T=318.15$ K			
NBA (1) + *n*-propanol (2)												
0.0797	1.268	−0.038	1.3795	0.0007					1.156	−0.021	1.3771	0.0005
0.1649	1.152	−0.075	1.3814	0.0010					1.056	−0.051	1.3791	0.0009
0.2522	1.056	−0.089	1.3832	0.0013					0.961	−0.074	1.3809	0.0011
0.3457	0.947	−0.111	1.3851	0.0015					0.865	−0.094	1.3828	0.0013
0.4374	0.835	−0.137	1.3868	0.0015					0.774	−0.109	1.3846	0.0014
0.5359	0.741	−0.139	1.3885	0.0015					0.685	−0.117	1.3864	0.0013
0.6415	0.649	−0.132	1.3903	0.0014					0.599	−0.116	1.3883	0.0013
0.7509	0.565	−0.114	1.3920	0.0011					0.525	−0.100	1.3900	0.0009
0.8682	0.499	−0.070	1.3936	0.0006					0.464	−0.064	1.3917	0.0005
0.9339	0.471	−0.037	1.3945	0.0003					0.439	−0.035	1.3927	0.0002
$T=298.15$ K					$T=303.15$ K				$T=308.15$ K			
NBA (1) + *sec*−propanol (2)												
0.0835	1.789	−0.153	1.3793	0.0022	1.564	−0.115	1.3728	0.0019	1.343	−0.114	1.3745	0.0017
0.1687	1.542	−0.270	1.3827	0.0036	1.332	−0.238	1.3767	0.0034	1.149	−0.216	1.3781	0.0031
0.2577	1.303	−0.374	1.3860	0.0048	1.134	−0.322	1.3802	0.0043	0.981	−0.289	1.3812	0.0039
0.3484	1.102	−0.436	1.3887	0.0053	0.999	−0.342	1.3833	0.0048	0.866	−0.307	1.384	0.0044
0.4400	0.957	−0.442	1.3912	0.0057	0.890	−0.334	1.3861	0.0050	0.771	−0.304	1.3864	0.0044
0.5459	0.857	−0.381	1.3937	0.0057	0.788	−0.301	1.3892	0.0050	0.692	−0.270	1.3889	0.0042
0.6470	0.781	−0.303	1.3959	0.0055	0.705	−0.255	1.3919	0.0048	0.632	−0.222	1.3911	0.0037
0.7580	0.689	−0.226	1.3980	0.0049	0.626	−0.193	1.3948	0.0045	0.567	−0.168	1.3933	0.0031
0.8753	0.592	−0.144	1.3995	0.0037	0.558	−0.111	1.3968	0.0032	0.509	−0.100	1.3956	0.0023
0.9352	0.548	−0.097	1.3999	0.0026	0.517	−0.076	1.3969	0.0016	0.482	−0.063	1.3962	0.0014
$T=313.15$ K									$T=318.15$ K			
NBA (1) + *sec*−propanol (2)												
0.0835	1.162	−0.109	1.3725	0.0015					1.031	−0.083	1.3696	0.0012
0.1687	1.004	−0.190	1.3760	0.0027					0.885	−0.164	1.3733	0.0025
0.2577	0.859	−0.255	1.3789	0.0032					0.776	−0.206	1.3762	0.0030
0.3484	0.765	−0.267	1.3815	0.0034					0.691	−0.222	1.3789	0.0032
0.4400	0.688	−0.262	1.3840	0.0035					0.617	−0.227	1.3814	0.0032
0.5459	0.612	−0.243	1.3867	0.0034					0.552	−0.212	1.3842	0.0030
0.6470	0.562	−0.202	1.3891	0.0031					0.501	−0.186	1.3869	0.0029
0.7580	0.507	−0.157	1.3916	0.0026					0.468	−0.135	1.3896	0.0026
0.8753	0.465	−0.093	1.3939	0.0018					0.449	-0.065	1.3919	0.0016

Table 3 (continued)

T=313.15 K					T=318.15 K			
0.9352	0.451	−0.053	1.3949	0.0012	0.435	−0.034	1.3931	0.0012

T=298.15 K				T=303.15 K				T=308.15 K			

NBA (1)+*n*-butanol (2)

0.1008	2.258	−0.099	1.3971	0.0002	2.022	−0.096	1.3949	0.0002	1.820	−0.084	1.3931	0.0001
0.1960	1.957	−0.208	1.3974	0.0003	1.778	−0.170	1.3953	0.0003	1.598	−0.155	1.3935	0.0002
0.2942	1.691	−0.276	1.3977	0.0004	1.527	−0.245	1.3956	0.0003	1.387	−0.210	1.3939	0.0002
0.3783	1.496	−0.302	1.3979	0.0004	1.359	−0.263	1.3958	0.0003	1.232	−0.231	1.3943	0.0003
0.4755	1.309	−0.293	1.3981	0.0004	1.181	−0.267	1.3961	0.0003	1.082	−0.227	1.3947	0.0003
0.5763	1.125	−0.274	1.3983	0.0004	1.035	−0.233	1.3964	0.0003	0.946	−0.203	1.3951	0.0003
0.6872	0.956	−0.220	1.3985	0.0003	0.877	−0.192	1.3966	0.0003	0.806	−0.167	1.3955	0.0002
0.7869	0.795	−0.180	1.3986	0.0002	0.733	−0.158	1.3968	0.0002	0.686	−0.128	1.3958	0.0002
0.8942	0.623	−0.136	1.3987	0.0001	0.595	−0.104	1.3970	0.0001	0.559	−0.085	1.3962	0.0001
0.9323	0.596	−0.086	1.3987	0.0000	0.562	−0.069	1.3971	0.0000	0.521	−0.063	1.3963	0.0000

T=313.15 K					T=318.15 K			

NBA (1)+*n*-butanol (2)

0.1008	1.573	−0.077	1.3913	0.0001	1.464	−0.069	1.3894	0.0001
0.1960	1.382	−0.141	1.3918	0.0002	1.291	−0.124	1.3899	0.0002
0.2942	1.206	−0.185	1.3923	0.0002	1.141	−0.153	1.3904	0.0002
0.3783	1.085	−0.193	1.3927	0.0002	1.028	−0.162	1.3909	0.0002
0.4755	0.953	−0.195	1.3932	0.0002	0.906	−0.163	1.3914	0.0002
0.5763	0.843	−0.170	1.3937	0.0002	0.795	−0.150	1.3918	0.0002
0.6872	0.719	−0.146	1.3941	0.0002	0.679	−0.128	1.3924	0.0002
0.7869	0.617	−0.114	1.3946	0.0002	0.581	−0.103	1.3928	0.0001
0.8942	0.516	−0.072	1.3950	0.0001	0.489	−0.062	1.3932	0.0001
0.9323	0.486	−0.051	1.3951	0.0000	0.457	−0.047	1.3934	0.0000

T=298.15 K				T=303.15 K				T=308.15 K			

NBA (1)+*sec*-butanol (2)

0.0964	2.564	−0.260	1.3957	0.0002	2.114	−0.201	1.3938	0.0001	1.776	−0.194	1.3918	0.0001
0.1944	2.156	−0.421	1.3961	0.0003	1.780	−0.339	1.3943	0.0002	1.489	−0.319	1.3924	0.0002
0.2863	1.837	−0.508	1.3965	0.0003	1.517	−0.419	1.3947	0.0003	1.279	−0.377	1.3929	0.0002
0.3879	1.553	−0.536	1.3969	0.0003	1.273	−0.460	1.3951	0.0003	1.101	−0.387	1.3935	0.0002
0.4788	1.348	−0.512	1.3972	0.0003	1.093	−0.458	1.3955	0.0003	0.971	−0.367	1.3940	0.0002
0.5914	1.134	−0.442	1.3976	0.0003	0.912	−0.414	1.3959	0.0003	0.841	−0.310	1.3946	0.0002
0.6785	0.990	−0.366	1.3979	0.0003	0.798	−0.354	1.3962	0.0003	0.749	−0.258	1.3950	0.0002
0.7826	0.828	−0.266	1.3983	0.0003	0.686	−0.258	1.3966	0.0002	0.645	−0.190	1.3955	0.0002
0.8902	0.674	−0.149	1.3986	0.0002	0.597	−0.132	1.3969	0.0001	0.546	−0.112	1.3960	0.0001
0.9310	0.621	−0.099	1.3987	0.0001	0.564	−0.084	1.3970	0.0000	0.516	−0.074	1.3962	0.0000

T=313.15 K					T=318.15 K			

NBA (1)+*sec*-butanol (2)

0.0964	1.483	−0.169	1.3899	0.0001	1.262	−0.165	1.3879	0.0001
0.1944	1.238	−0.283	1.3906	0.0002	1.057	−0.261	1.3886	0.0001
0.2863	1.039	−0.360	1.3912	0.0002	0.916	−0.300	1.3892	0.0001
0.3879	0.899	−0.364	1.3918	0.0002	0.799	−0.303	1.3899	0.0002
0.4788	0.801	−0.341	1.3924	0.0002	0.717	−0.284	1.3905	0.0002
0.5914	0.706	−0.285	1.3931	0.0002	0.629	−0.247	1.3912	0.0002
0.6785	0.637	−0.238	1.3936	0.0002	0.567	−0.211	1.3918	0.0002
0.7826	0.559	−0.177	1.3942	0.0001	0.498	−0.164	1.3924	0.0001

Table 3 (continued)

T = 313.15 K					T = 318.15 K			
0.8902	0.488	− 0.105	1.3948	0.0001	0.441	− 0.101	1.3930	0.0001
0.9310	0.467	− 0.071	1.3950	0.0000	0.427	− 0.070	1.3933	0.0000

T = 298.15 K					T = 303.15 K				T = 308.15 K			
NBA (1) + *iso*-butanol (2)												
0.0981	3.029	− 0.101	1.3953	0.0009	2.591	− 0.097	1.3929	0.0008	2.199	− 0.091	1.3904	0.0008
0.1955	2.621	− 0.230	1.3961	0.0012	2.246	− 0.207	1.3938	0.0011	1.921	− 0.173	1.3915	0.0011
0.2890	2.295	− 0.288	1.3966	0.0013	1.971	− 0.256	1.3944	0.0013	1.688	− 0.218	1.3923	0.0012
0.3929	1.968	− 0.317	1.3972	0.0013	1.691	− 0.285	1.3950	0.0013	1.454	− 0.243	1.3931	0.0012
0.4885	1.703	− 0.308	1.3976	0.0013	1.472	− 0.273	1.3955	0.0012	1.260	− 0.245	1.3938	0.0012
0.5869	1.447	− 0.282	1.3980	0.0012	1.266	− 0.242	1.3960	0.0012	1.081	− 0.226	1.3945	0.0011
0.6843	1.217	− 0.233	1.3983	0.0010	1.068	− 0.204	1.3964	0.0010	0.914	− 0.197	1.3950	0.0009
0.7820	0.975	− 0.195	1.3984	0.0006	0.871	− 0.165	1.3966	0.0006	0.772	− 0.142	1.3954	0.0006
0.8913	0.719	− 0.139	1.3986	0.0003	0.675	− 0.098	1.3968	0.0002	0.611	− 0.084	1.3959	0.0002
0.9456	0.614	− 0.088	1.3987	0.0001	0.562	− 0.079	1.3970	0.0001	0.522	− 0.063	1.3962	0.0001

T = 313.15 K					T = 318.15 K			
NBA (1) + *iso*-butanol (2)								
0.0981	1.908	− 0.086	1.3883	0.0007	1.649	− 0.072	1.3869	0.0006
0.1955	1.662	− 0.165	1.3895	0.0010	1.436	− 0.144	1.3881	0.0009
0.2890	1.468	− 0.198	1.3905	0.0012	1.274	− 0.171	1.3890	0.0011
0.3929	1.272	− 0.216	1.3914	0.0012	1.120	− 0.176	1.3899	0.0012
0.4885	1.105	− 0.219	1.3922	0.0012	0.987	− 0.171	1.3907	0.0012
0.5869	0.957	− 0.198	1.3929	0.0011	0.853	− 0.163	1.3913	0.0010
0.6843	0.803	− 0.185	1.3935	0.0008	0.722	− 0.153	1.3919	0.0008
0.7820	0.684	− 0.136	1.3940	0.0005	0.615	− 0.119	1.3924	0.0005
0.8913	0.552	− 0.081	1.3947	0.0002	0.507	− 0.070	1.3930	0.0002
0.9456	0.484	− 0.055	1.3950	0.0001	0.459	− 0.039	1.3933	0.0001

Standard uncertainties *u*: *u* (T) = 0.01 K; *u(p)* = 0.04 MPa; *u(η)* = 0.003 mPa s; *u(n_D)* = 0.0005; (level of confidence = 95%, *k* = 2).
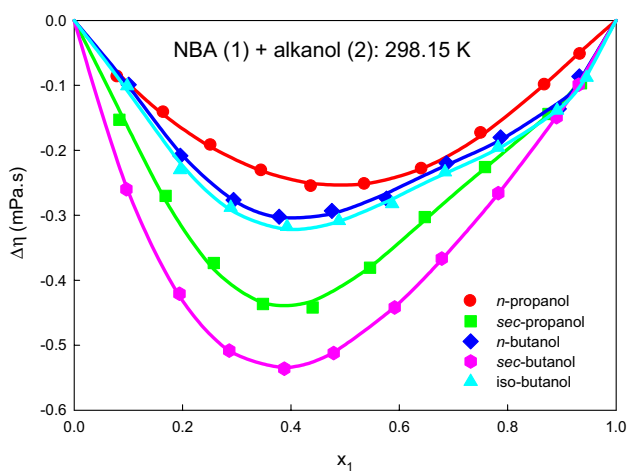
$$\Delta \eta = \eta_{\text{mix}} - \sum_i x_i \eta_i \tag{1}$$

Here η_{mix} and η_i are the η data of binary mixtures and pure components.

To fit the $\Delta\eta$ data, the RK equation [Eq. (2)] was employed.

$$X\left(\Delta \eta \text{ or } \Delta n_D\right) = x_1\left(1 - x_1\right)\left[\sum_{j=1}^{4} A^{(j)}\left(2x_1 - 1\right)^{j-1}\right] \tag{2}$$

where $A^{(j)}$ symbolize adjustable parameters reported in Table 4 along with standard deviation $\sigma(X)$ given by the equation.
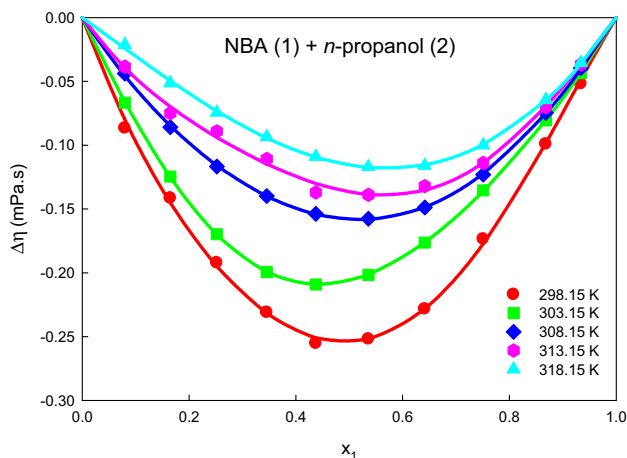
$$\sigma(X) = \left(\frac{\sum \left(X_{\text{exptl}} - X_{\text{calcd.}}\right)^2}{(m - n))}\right)^{1/2} \tag{3}$$

Fig. 1 Deviation in viscosity ($\Delta\eta$) as a function of mole fraction of NBA (x_1), where symbols represent experimental data and lines represent values calculated from the Redlich–Kister equation

Table 4 Adjustable parameters for deviation in viscosity ($\Delta\eta$/mPa · s) and deviation in refractive index (Δn_D) along with standard deviations (σ)

Property	T/K	$A^{(1)}$	$A^{(2)}$	$A^{(3)}$	$A^{(4)}$	σ
NBA (1)+n-propanol (2)						
$\Delta\eta$/mPa s	298.15	−1.016	0.041	0.097	0.182	0.004
	303.15	−0.825	0.206	0.037	−0.126	0.001
	308.15	−0.633	−0.049	−0.007	0.044	0.001
	313.15	−0.547	−0.151	−0.027	0.165	0.004
	318.15	−0.463	−0.140	0.011	−0.014	0.001
Δn_D	298.15	0.0084	−0.0007	0.0045	−0.0066	0.0084
	303.15	0.0074	−0.0024	0.0014	−0.0009	0.0074
	308.15	0.0066	−0.0010	0.0011	−0.0016	0.0066
	313.15	0.0060	−0.0006	0.0010	−0.0025	0.0060
	318.15	0.0055	−0.0005	−0.0002	−0.0026	0.0055
NBA (1)+sec-propanol (2)						
$\Delta\eta$/mPa s	298.15	−1.629	1.059	0.016	−1.192	0.009
	303.15	−1.291	0.781	−0.155	−0.709	0.008
	308.15	−1.153	0.726	−0.169	−0.580	0.004
	313.15	−1.016	0.525	−0.218	−0.277	0.004
	318.15	−0.894	0.311	−0.004	0.084	0.005
Δn_D	298.15	0.0225	−0.0007	0.0145	0.0103	0.0225
	303.15	0.0203	0.0010	0.0109	0.0017	0.0203
	308.15	0.0171	−0.0057	0.0078	0.0079	0.0171
	313.15	0.0137	−0.0035	0.0082	0.0033	0.0137
	318.15	0.0126	−0.0029	0.0077	0.0036	0.0126
NBA (1)+n-butanol (2)						
$\Delta\eta$/mPa s	298.15	−1.167	0.542	−0.114	−1.077	0.006
	303.15	−1.029	0.440	−0.015	−0.773	0.005
	308.15	−0.889	0.406	−0.016	−0.638	0.002
	313.15	−0.757	0.327	−0.090	−0.424	0.002
	318.15	−0.640	0.208	−0.147	−0.221	0.002
Δn_D	298.15	0.0017	0.0000	0.0000	−0.0011	0.0017
	303.15	0.0013	0.0000	0.0002	−0.0010	0.0013
	308.15	0.0011	0.0000	0.0001	−0.0009	0.0011
	313.15	0.0010	0.0001	0.0001	−0.0009	0.0010
	318.15	0.0009	0.0000	0.0000	−0.0007	0.0009
NBA (1)+sec-butanol (2)						
$\Delta\eta$/mPa s	298.15	−2.003	1.041	−0.343	−0.247	0.002
	303.15	−1.814	0.522	−0.022	0.112	0.001
	308.15	−1.427	0.855	−0.393	−0.281	0.001
	313.15	−1.309	0.762	−0.311	−0.351	0.009
	318.15	−1.113	0.619	−0.559	−0.144	0.000
Δn_D	298.15	0.0014	−0.0001	0.0010	−0.0007	0.0014
	303.15	0.0013	−0.0002	0.0000	−0.0003	0.0013
	308.15	0.0009	0.0000	0.0001	−0.0006	0.0009
	313.15	0.0009	−0.0001	0.0000	−0.0004	0.0009
	318.15	0.0008	0.0001	−0.0001	−0.0007	0.0008
NBA (1)+iso-butanol (2)						
$\Delta\eta$/mPa · s	298.15	−1.226	0.588	−0.187	−1.149	0.006
	303.15	−1.083	0.550	−0.110	−0.856	0.008
	308.15	−0.971	0.287	−0.024	−0.342	0.007
	313.15	−0.866	0.222	−0.145	−0.216	0.006
	318.15	−0.703	0.178	−0.221	−0.120	0.007

Table 4 (continued)

Property	T/K	$A^{(1)}$	$A^{(2)}$	$A^{(3)}$	$A^{(4)}$	σ
Δn_D	298.15	0.0051	− 0.0017	0.0019	− 0.0044	0.0051
	303.15	0.0050	− 0.0014	0.0010	− 0.0043	0.0050
	308.15	0.0048	− 0.0016	0.0007	− 0.0038	0.0048
	313.15	0.0047	− 0.0023	− 0.0002	− 0.0019	0.0047
	318.15	0.0046	− 0.0022	− 0.0006	− 0.0015	0.0046

Fig. 2 Deviation in viscosity ($\Delta\eta$) as a function of mole fraction of NBA (x_1), where symbols represent experimental data and lines represent values calculated from the Redlich–Kister equation

Fig. 3 Excess Gibbs free energy of activation (ΔG^{*E}) as a function of mole fraction of NBA (x_1), where symbols represent experimental data and lines represent values calculated from Redlich–Kister equation

Here m and n represent the number of experimental points and adjustable parameters ($j-1$), respectively.

The $\Delta\eta$ versus x_1 values were found to be negative over the entire composition range for the present binary mixtures as represented in Fig. 1 and negative values of $\Delta\eta$ follow the sequence: *n*-propanol > *n*-butanol > *iso*-butanol > *sec*-propanol > *sec*-butanol. The $\Delta\eta$ values increase with an increase in temperature for all the NBA (1) + alkanol (2) systems (Fig. 2).

The viscosity of a mixture depends upon the structure of molecules and molecular interactions among, unlike molecules. If the deviation in viscosity between the binary liquid mixtures shows a positive contribution, it indicates strong interactions, whereas the negative contribution shows the mixtures without specific interactions [41]. Thus, in the present systems, the negative $\Delta\eta$ of the mixtures cannot explain the strong interactions between the NBA and alcohol. This confirms that the strength of intermolecular hydrogen bonding is not the only factor affecting the $\Delta\eta$ of these mixtures but the size and shape of the molecules (NBA and alkanol) play a vital role. The excess free energy of activation (ΔG^{*E}) is also considered a reliable criterion to detect or exclude the presence of interactions between the binary liquid mixtures. The positive

ΔG^{*E} values indicate specific interactions, while negative values indicate the dominance of dispersion forces [42]. For this binary ($A + B$) system, ΔG^{*E} is negative over the entire composition range (Fig. 3). This further confirms the dominance of dispersion forces in these binary systems. The increase in temperature weakens the intermolecular association due to the rise in the kinetic energy of molecules, thus resulting in decreased viscosity [43].

Ab Initio Approach

In this paper, we utilized an Ab initio approach that not only characterizes the $\Delta\eta$ of binary mixtures containing associated components but also provides insights into intermolecular interactions. Since both components (1 and 2) of binary mixtures are self-associated through hydrogen bonding, these components are assumed to exist in polymeric form and are expressed as 1_n and 2_n.

The utilized approach assumes that the $\Delta\eta$ values for the present NBA (1) + alkanol (2) mixtures are the viscosity change caused by the following three processes (a), (b), and (c):

The formation of (1_n)–(2_n) interactions between the NBA (1) and alkanol (2) exist as self-associated (1_n and 2_n), with an interactional parameter of $\chi_{12}^{\dagger}$ per mole.

$$\Delta\eta_a = x_1\chi_{12}^{\dagger}S_2 \qquad (4)$$

$$S_2 = \frac{x_2 V_2}{\sum x_1 V_1} \qquad (5)$$

Here S_2 represents the surface fraction of alkanol in (1_n)–(2_n) interaction [44, 45].

These (1_n)–(2_n) interactions lead to the rupturing/depolymerization of (i) intermolecular association (H-bonding) in pure NBA and alkanol molecules to produce their monomers with interactional parameter as χ_{11} and χ_{22} per mole.

$$\Delta\eta_{b(i)} = x_1\chi_{11}S_2' \qquad (6)$$

$$\Delta\eta_{b(ii)} = x_1\chi_{22}S_2' \qquad (7)$$

$$S_2' \propto x_1 S_2 = \frac{K x_1 x_2 V_2}{\sum x_i V_i} \qquad (8)$$

Here S_2' is referred to as the alkanol surface fraction that causes the NBA changes.

The monomers of NBA and alkanol would then interact with each other to form (1)–(2) interactions with interactional energy parameters as χ_{12} per mole.

$$\Delta\eta_c = \chi_{12}S_2' x_2 \qquad (9)$$

Therefore, the total change in η ($\Delta\eta$) including all three processes (a), (b), and (c) is estimated as

$$\Delta\eta = \left[\frac{x_1 x_2 V_2}{\sum x_i V_i}\right]\left[\chi_{12}^* + K x_1 \chi_{11} + K x_1 \chi_{22} + K x_2 \chi_{12}\right] \qquad (10)$$

Since both the components of the current mixtures are self-associated through hydrogen bonding, it is reasonable to assume that.

$\chi_{12}^{\dagger} = K\chi_{12} = \chi_{12}^*$ and $K\chi_{11} = K\chi_{22} = \chi^*$ so Eq. (10) reduces to

$$\Delta\eta = \left[\frac{x_1 x_2 V_2}{\sum x_i V_i}\right]\left[\chi_{12}^*(1 + x_2) + x_1\chi^*\right] \qquad (11)$$

The experimental values at two compositions ($x_1 \approx 0.5$ and 0.6) were used to compute parameters χ_{12}^* and χ^* from Eq. (11) and represented in Table 6. Using these χ_{12}^* and χ^* parameters, the $\Delta\eta$ values were calculated at other mole fractions and are shown in Fig. 4. The prediction capability of this approach is expressed as standard deviations in Table 5. Since χ^* is a measure of the extent of depolymerization of NBA or alkanol upon mixing, the
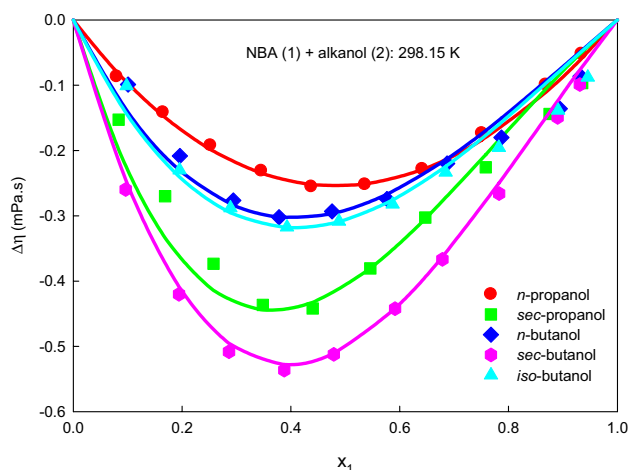
Fig. 4 Deviation in viscosity ($\Delta\eta$) as a function of mole fraction of NBA (x_1) where symbols represent experimental data and lines represent the values predicted through the Ab initio approach

magnitude of χ^*, as shown in Table 6, indicates that maximum depolymerization occurs with *n*-propanol. Moreover, the magnitude of χ_{12}^*, which is a measure of unlike interactions between NBA and alkanol, reveals that *n*-propanol and *n*-butanol interacts strongly with NBA compared to other alkanol and weakly with *sec*-butanol. This may be due to the two –CH_2 groups attached to the C atom involved with hydroxyl oxygen which offers steric hindrance and restrict the proper orientation of –OH required for the interaction with the amine group.

Correlations for Viscosity

The viscosity of the binary mixtures was predicted by following four correlations employing the experimental pure components viscosity (η) data and results are demonstrated in Fig. 5 [13, 46–49] and prediction ability of these correlations were expressed in terms of $\sigma(\eta)$, as presented in Table 5.

Grunberg and Nissan [50]

$$\eta = \exp\left[\sum_{i=1,2}(x_i \ln \eta_i) + G_{12}\prod_{i=1,2}x_i\right] \qquad (12)$$

Here, G_{12} is Grunberg-Nissan interactional parameter, with the results shown in Table 6. Positive G_{12} values imply stronger specific interactions in butanol mixtures, while a negative G_{12} value indicates relatively weaker interactions in propanol mixtures.

Table 5 Standard deviations for viscosity (η) and refractive index (n_D) for binary systems calculated by using various correlations at $T = 298.15$ K

Correlation	System				
	NBA + *n*-propanol	NBA + *sec*-propanol	NBA + *n*-butanol	NBA + *sec*-butanol	NBA + *iso*-butanol
Grunberg and Nissan (Eq. 12)	0.169	0.096	0.306	0.321	0.565
Tamura and Kurata (Eq. 13)	0.008	0.040	0.023	0.075	0.027
Hind, McLaughlin, and Ubbelohde (Eq. 14)	0.009	0.053	0.025	0.080	0.029
Katti and Chaudhari (Eq. 15)	0.035	0.045	0.044	0.044	0.061
Ab initio approach (Eq. 11)	0.006	0.034	0.028	0.014	0.029
Arago–Biot (Eq. 17)	0.0011	0.0042	0.0003	0.0003	0.0012
Gladstone–Dale (Eq. 18)	0.0011	0.0042	0.0003	0.0003	0.0012
Lorentz–Lorentz (Eq. 19)	0.0011	0.0042	0.0003	0.0003	0.0012
Wernier (Eq. 20)	0.0010	0.0039	0.0003	0.0003	0.0011
Heller (Eq. 21)	0.0011	0.0042	0.0003	0.0003	0.0012
Newton (Eq. 22)	0.0011	0.0041	0.0003	0.0003	0.0012
Erying (Eq. 23)	0.0011	0.0042	0.0003	0.0003	0.0012

Table 6 Interactional parameters based on various models/correlations for NBA (1) + alkanol (2) calculated by various correlations at $T = 298.15$ K

Correlations	Parameter	System				
		NBA + *n*-propanol	NBA + *sec*-propanol	NBA + *n*-butanol	NBA + *sec*-butanol	NBA + *iso*-butanol
Ab initio approach (Eq. 11)	χ_{12}^*	− 0.548	− 1.409	− 0.832	− 1.503	− 0.863
	χ^*	− 0.708	0.502	0.075	0.362	0.154
Grunberg and Nissan (Eq. 12)	G_{12}	− 4.188	− 0.641	0.208	0.048	0.800
Tamura and Kurata (Eq. 13)	T_{12}	0.874	0.587	0.988	0.819	1.388
Hind, McLaughlin, and Ubbelohde (Eq. 14)	H_{12}	0.579	0.260	0.943	0.692	1.875
Katti and Chaudhari (Eq. 15)	W_{vis}/RT	− 7005.84	− 8199.12	− 6050.87	− 6443.99	− 4499.14

Tamura and Kurata [51]

$$\eta = \left[\sum_{i=1,2} x_i \phi_i \eta_i + 2T_{12} \prod_{i=1,2} \left(x_i \phi_i \right)^{1/2} \right] \quad (13)$$

where T_{12} is *TK* interactional parameter as given in Table 6 and its value is positive for all the binary mixtures as shown in Fig. 5.

Hind, McLaughlin, and Ubbelohde [52]

$$\eta = \left[\sum_{i=1,2} x_i^2 \eta_i + 2H_{12} \prod_{i=1,2} x_i \right] \quad (14)$$

where H_{12} is the Hind interactional parameter shown in Table 6 and all of the binary systems studied show positive values, indicating favorable interactions as presented in Fig. 5.

Katti and Chaudhari [53, 54]

$$\ln \eta V_m = \sum_{i=1,2} x_i \ln \left(\eta_i V_i \right) + x_1 x_2 \left(W_{\text{vis}}/RT \right) \quad (15)$$

The interactional energy parameter value of W_{vis}/RT is given in Table 6 and correlated data results are shown in Fig. 5.

The η values were predicted using various correlations and analyzed using standard deviation. The values of $\sigma(\eta)$ for these correlations [Eqs. (11), (13)–(15)] were found to
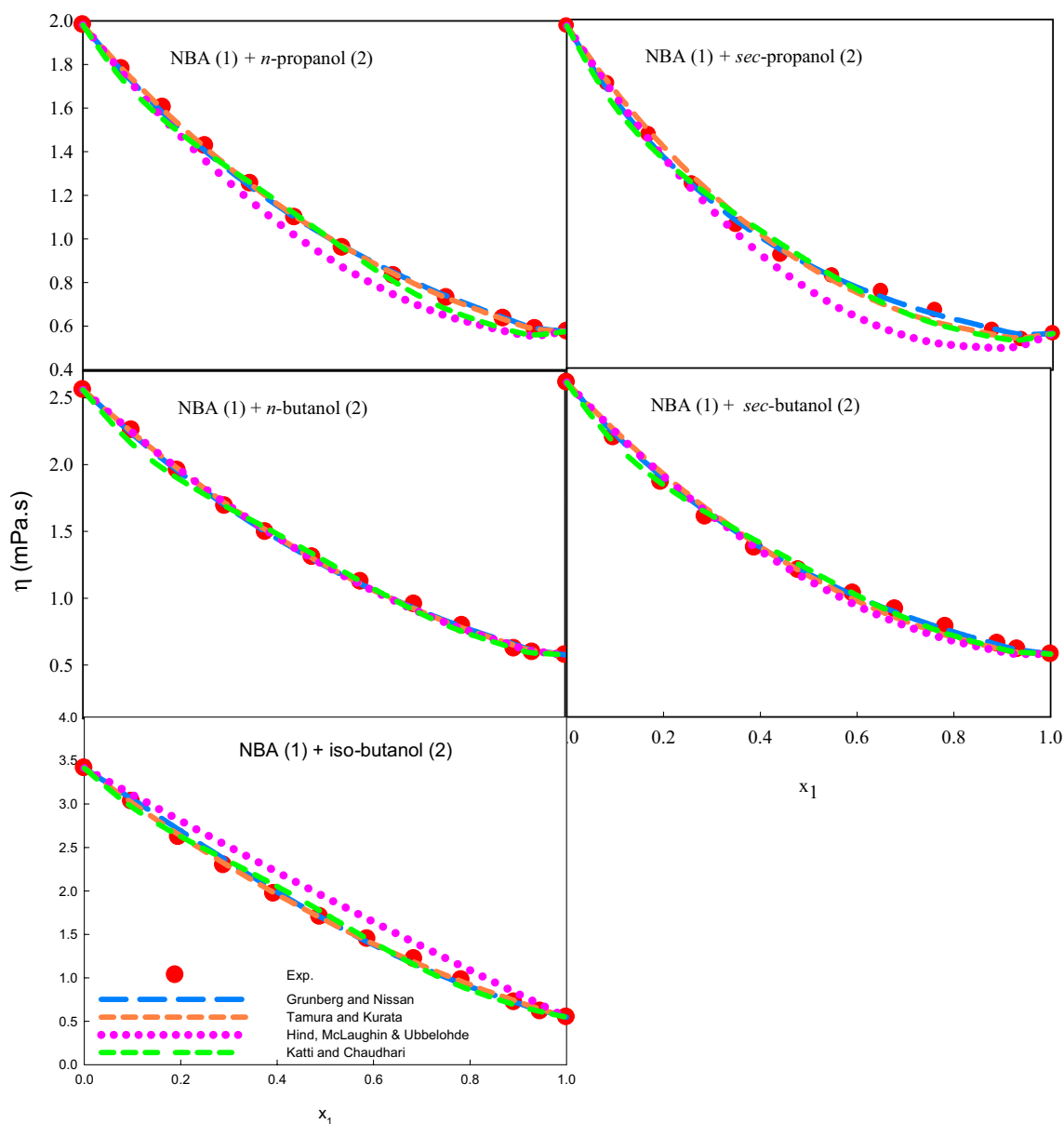
Fig. 5 Viscosity (η) as a function of mole fraction of NBA (x_1), predicted by various correlations at 298.15 K

be in the range of 0.006–0.088, whereas for Grunberg and Nissan correlation, it varies in the range of 0.096- 0.565 for the present NBA + alkanol systems.
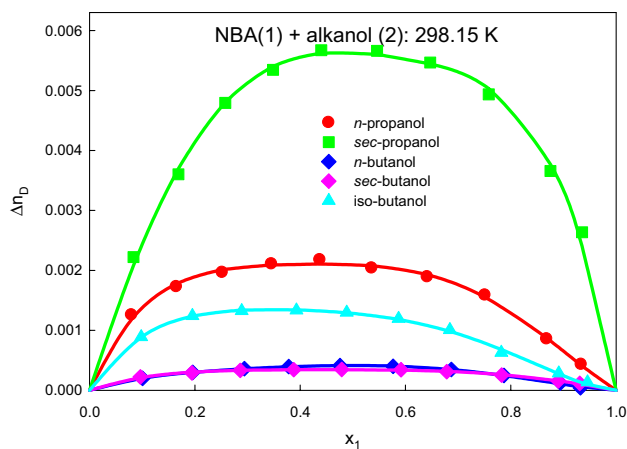
Refractive Index

The (Δn_D) values were calculated as follows:

$$\Delta n_D = n_D - \sum_{i=1}^{2} x_i n_{Di} \qquad (16)$$

The measured n_D and Δn_D data of NBA (1) + alkanol (2) systems are presented in Table 3 and depicted as Δn_D versus x_1 in Fig. 6. The adjustable parameters $A^{(j)}$ along with standard deviations $\sigma(\Delta n_D)$ were calculated by using RK equation (Table 4).

The Δn_D values for binary systems are positive and follow the sequence: *sec*-propanol > *n*-propanol > *iso*-butanol > *n*-butanol > *sec*-butanol, as demonstrated in Fig. 6. The observed positive values of Δn_D values can be attributed to the formation of specific hydrogen bonding interaction between (–OH) of alkanols and NH_2 group of the amine. The amine has a lone pair electron in *p*-orbitals, which readily interacts with the acidic hydrogen of the –OH group in alkanols [55–57]. As shown in Fig. 6, the

Fig. 6 Deviation in refractive index (Δn_D) as a function of mole fraction of NBA (x_1), where symbols represent experimental data and lines represent values calculated from the Redlich–Kister equation
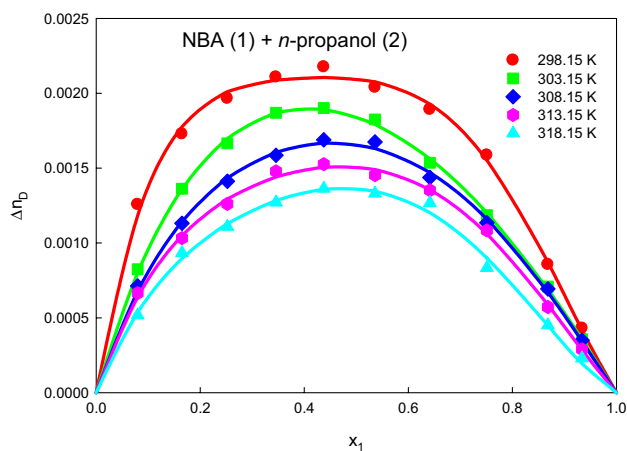
Fig. 7 Deviation in refractive index (Δn_D) as a function of mole fraction of NBA (x_1), where symbols represent experimental data and lines represent values calculated from the Redlich–Kister equation

Δn_D values decrease with an increase in the chain length of alkanol molecules [55]. This trend may be due to a decrease in the acidity of the –OH group resulting from the addition of an alkyl group, which ultimately leads to a reduction in the specific interaction between the component molecules. The Δn_D values for NBA (1) + *sec*-propanol (2) are higher as compared to NBA (1) + *sec*-butanol (2), which may be due to the larger size of the butanol molecule providing more steric hindrance and forming intermolecular associations. In contrast, the smaller size of the propanol allows it to interact more easily with NBA molecules, resulting in higher excess refractive index values. In this study, we also examined the effect of temperature on n_D; as the temperature increases, the Δn_D data for NBA (1) + alkanol (2) mixtures decrease, as demonstrated

in Fig. 7, indicating a weakening of intermolecular interactions between the components of the mixture.

The n_D data were calculated using the following mixing rules [19] and then compared using standard deviation (σ) at all temperatures as shown in Table 5:

$$\text{Arago} - \text{Biot (A} - \text{B)} \quad n_D = n_{D1}\phi_1 + n_{D2}\phi_2 \quad (17)$$

$$\text{Gladstone} - \text{Dale (G} - \text{D)} \quad n_D - 1 = (n_{D1} - 1)\phi_1 + (n_{D2} - 1)\phi_2 \quad (18)$$

$$\text{Lorentz} - \text{Lorenz (L} - \text{L)} \quad \frac{n_D^2 - 1}{n_D^2 + 2}$$
$$= \left(\frac{n_{D1}^2 - 1}{n_D^2 + 2}\right)\phi_1 + \left(\frac{n_{D2}^2 - 1}{n_D^2 + 2}\right)\phi_2 \quad (19)$$

$$\text{Heller (H)} \quad \frac{n_D - 1}{n_D} = \frac{3}{2}\left(\frac{(n_{D2}/n_{D1})^2 - 1}{(n_{D2}/n_{D1})^2 + 2}\right)\phi_2 \quad (20)$$

$$\text{Weiner (W)} \quad \frac{n_D^2 - n_{D1}^2}{n_D^2 + 2n_{D2}^2} = \left(\frac{n_{D2}^2 - n_{D1}^2}{n_{D2}^2 + 2n_{D2}^2}\right)\phi_2 \quad (21)$$

$$\text{Newton (Nw)} \quad n_D^2 - 1 = \left(n_{D1}^2 - 1\right)\phi_1 + \left(n_{D2}^2 - 1\right)\phi_2 \quad (22)$$

$$\text{Erying and John (E} - \text{J)} \quad n_D = n_{D1}\phi_1^2 + 2\left(n_{D1}n_{D2}\right)^{1/2}\phi_1\phi_2 + n_{D2}\phi_2^2 \quad (23)$$

In these equations, n_D, n_{D1} and n_{D2} represent the refractive index of mixture and pure compounds, respectively.

The values of n_D for these binary mixtures predicted from above Eqs. (17)-(23) are shown in Fig. 8. All the correlations predict similar values of refractive index (Fig. 8) of mixtures as these plots are overlapping and indistinguishable. This is because the present mixtures are highly non-ideal due to like (*i–i*) and unlike (*i–j*) intermolecular interaction (hydrogen bonding) and therefore, these correlations are not very impressive to correlate such types of associated mixtures. The difference in experimental and predictive values are shown in terms of standard deviations [calculated from Eq. (3)] in Table 5. Similar behavior was also reported in the literature for associated binary mixtures [19, 20, 58, 59].

Conclusions

In conclusion, we investigated viscosity and refractive index properties in NBA + alkanol mixtures over a temperature range $T = (298.15–318.15$ K) and at pressure 0.1 MPa over the entire composition range. The sequence of viscosity
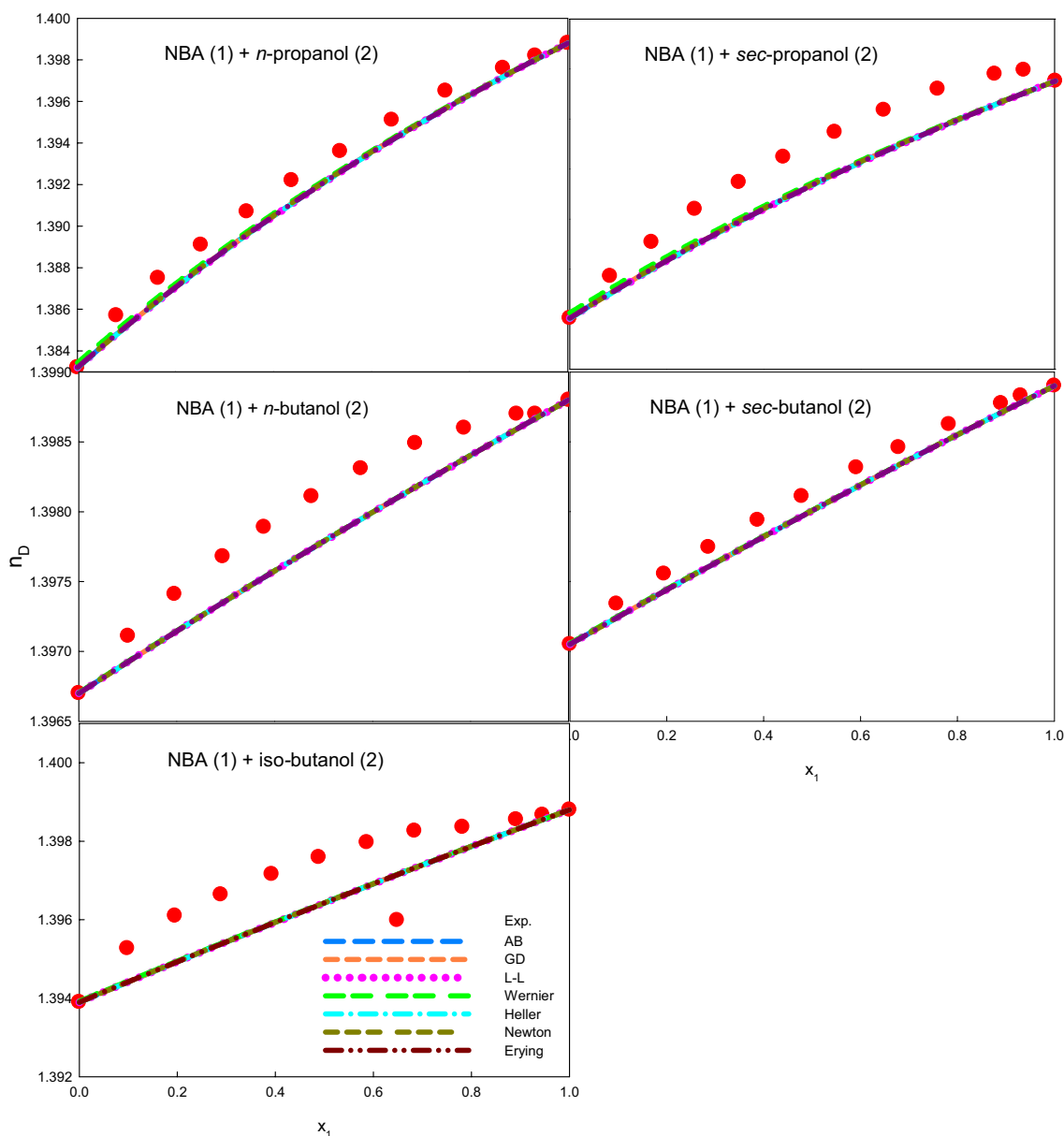
Fig. 8 Refractive index (n_D) as a function of mole fraction of NBA (x_1), predicted by various correlations at 298.15 K

deviation $\Delta\eta$ follows the trend: *n*-propanol > *n*-butanol > *iso*-butanol > *sec*-propanol > *sec*-butanol, which reveals the unlike interactions were stronger in the case of *n*-propanol, resulting in the maximum deviation, while *sec*-butanol exhibited the lowest deviation due to steric hindrance. Additionally, the *Ab-initio* approach was employed to determine the $\Delta\eta$ values, and various correlations were used to predict the viscosity data at 298.15 K.

This study contributes to the parameters required for CO_2 capture by blended absorbents, a critical technology for reducing carbon emissions. Amines, commonly used solvents for capturing CO_2, were combined with

alkanols as the second component to enhance amine solubility through hydrogen bonding. The refractive indices (n_D) of NBA with alkanol binary systems were studied and exhibited positive Δn_D values with the sequence: *sec*-propanol > *n*-propanol > *iso*-butanol > *n*-butanol > *sec*-butanol, indicating specific hydrogen bonding interactions between the hydroxyl (–OH) group of alkanol and –NH₂ group of amines.

References

1. S. Gössling, S. Dolnicar, WIREs Clim. Change **14**, e802 (2023)
2. N. Cahill, Significance **15**, 24 (2018)
3. X. Song, F. Wang, D. Ma, M. Gao, Y. Zhang, Pet. Explor. Dev. **50**, 229 (2023)
4. M. Meinshausen, N. Meinshausen, W. Hare, S.C.B. Raper, K. Frieler, R. Knutti, D.J. Frame, M.R. Allen, Nature **458**, 1158 (2009)
5. M. Herrero, P. Gerber, T. Vellinga, T. Garnett, A. Leip, C. Opio, H.J. Westhoek, P.K. Thornton, J. Olesen, N. Hutchings, H. Montgomery, J.F. Soussana, H. Steinfeld, T.A. McAllister, Anim. Feed Sci. Technol. **166–167**, 779 (2011)
6. R.A. Kerr, Science **312**, 825 (2006)
7. D.Y.C. Leung, G. Caramanna, M.M. Maroto-Valer, Renew. Sustain. Energy Rev. **39**, 426 (2014)
8. S. Anderson, R. Newell, Ann. Rev. Environ. Resour. **29**, 109 (2004)
9. F. Bowen, Energy Policy **39**, 2256 (2011)
10. E. Nessi, A.I. Papadopoulos, P. Seferlis, Int. J. Greenhouse Gas Control **111**, 103474 (2021)
11. A. Afsharpour, S.H. Esmaeli-Faraj, Korean J. Chem. Eng. **39**, 1576 (2022)
12. F.A. Perdomo, S.H. Khalit, E.J. Graham, F. Tzirakis, A.I. Papadopoulos, I. Tsivintzelis, P. Seferlis, C.S. Adjiman, G. Jackson, A. Galindo, Fluid Phase Equilib. **566**, 113635 (2023)
13. S. Verma, P. Bhagat, S. Gahlyan, M. Rani, N. Kumar, R.K. Malik, Y. Lee, S. Maken, Korean J. Chem. Eng. (2023). https://doi.org/10.1007/s11814-023-1422-2
14. W.M. Budzianowski, Int. J. Global Warm. **7**, 184 (2015)
15. P.D. Vaidya, E.Y. Kenig, Chem. Eng. Technol. **30**, 1467 (2007)
16. M. Yiannourakou, X. Rozanska, B. Minisini, F. de Meyer, Fluid Phase Equilib. **560**, 113478 (2022)
17. M. Rani, S. Maken, S.J. Park, Korean J. Chem. Eng. **36**, 1401 (2019)
18. S. Gahlyan, P. Bhagat, R. Devi, S. Verma, M. Rani, S. Maken, J. Mol. Liq. **304**, 112740 (2020)
19. P. Bhagat, S. Maken, J. Mol. Liq. **323**, 114640 (2021)
20. S. Verma, S. Gahlyan, M. Rani, S. Maken, Korean Chem. Eng. Res. **56**, 663 (2018)
21. J.A. Riddick, W.B. Bunger, T.K. Sakano, *Organic Solvents. Physical Properties and Methods of Purification*, 4th edn. (Wiley, New York, 1986)
22. M. Domínguez, I. Gascón, A. Valén, F.M. Royo, J.S. Urieta, J. Chem. Thermodyn. **32**, 1551 (2000)
23. J.K. Shah, K.J. De Witt, C.E. Stoops, J. Chem. Eng. Data **14**, 333 (1969)
24. M. Domínguez, J. Pardo, M.C. López, F.M. Royo, J.S. Urieta, Fluid Phase Equilib. **124**, 147 (1996)
25. J.W. Bayles, T.M. Letcher, J. Chem. Eng. Data **16**, 266 (1971)
26. H.A. Zarei, S. Asadi, H. Iloukhani, J. Mol. Liq. **141**, 25 (2008)
27. C. Yang, H. Lai, Z. Liu, P. Ma, J. Chem. Eng. Data **51**, 1345 (2006)
28. J. Ortega, J. Chem. Eng. Data **27**, 312 (1982)
29. M. Rani, S. Maken, J. Ind. Eng. Chem. **18**, 1694 (2012)
30. F.-M. Pang, C.-E. Seng, T.-T. Teng, M.H. Ibrahim, J. Mol. Liq. **136**, 71 (2007)
31. C.-T. Yeh, C.-H. Tu, J. Chem. Eng. Data **52**, 1760 (2007)
32. M. Domínguez, S. Rodríguez, M.C. López, F.M. Royo, J.S. Urieta, J. Chem. Eng. Data **41**, 37 (1996)
33. S. Martínez, R. Garriga, P. Pérez, M. Gracia, Fluid Phase Equilib. **168**, 267 (2000)
34. A.K. Nain, J. Chem. Eng. Data **53**, 1208 (2008)
35. D.M. Majstorović, E.M. Živković, M.L. Kijevčanin, J. Chem. Eng. Data **62**, 275 (2017)
36. T.M. Aminabhavi, B. Gopalkrishna, J. Chem. Eng. Data **39**, 865 (1994)
37. S. Verma, S. Gahlyan, M. Rani, S. Maken, J. Mol. Liq. **265**, 468 (2018)
38. S. Gahlyan, N. Verma, S. Verma, M. Rani, S.-J. Park, S. Maken, J. Mol. Liq. **298**, 111946 (2020)
39. S. Verma, S. Gahlyan, J. Kaur, S. Maken, J. Mol. Liq. **292**, 111359 (2019)
40. S. Gahlyan, S. Verma, M. Rani, S. Maken, J. Mol. Liq. **244**, 233 (2017)
41. H. Vogel, A. Weiss, J. Phys. Chem. **86**, 193 (1982)
42. G.P. Dubey, K. Kumar, J. Chem. Eng. Data **61**, 1967 (2016)
43. G. Manukonda, V. Ponneri, S. Kasibhatta, S. Sakamuri, Korean J. Chem. Eng. **30**, 1131 (2013)
44. M.L. Huggins, Polymer **12**, 389 (1971)
45. M.L. Huggins, J. Phys. Chem. **74**, 371 (1970)
46. S. Verma, S. Gahlyan, P. Bhagat, M. Rani, M. Bhagat, S. Rana, V.K. Rattan, Y. Lee, S. Maken, J. Mol. Liq. **386**, 122498 (2023)
47. S. Verma, A. Sharma, S. Gahlyan, M. Rani, S. Maken, J. Mol. Liq. **387**, 122709 (2023)
48. S. Verma, P. Bhagat, S. Gahlyan, M. Rani, N. Kumar, R.K. Malik, Y. Lee, S. Maken, J. Mol. Liq. **382**, 121967 (2023)
49. S. Verma, M. Rani, Y. Lee, S. Maken, J. Mol. Liq. **387**, 122663 (2023)
50. L. Grunberg, A.H. Nissan, Nature **164**, 799 (1949)
51. M. Tamura, M. Kurata, Bull. Chem. Soc. Jpn **25**, 32 (1952)
52. R.K. Hind, E. McLaughlin, A.R. Ubbelohde, Trans. Faraday Soc. **56**, 328 (1960)
53. P.K. Katti, M.M. Chaudhri, J. Chem. Eng. Data **9**, 442 (1964)
54. P.K. Katti, M.M. Chaudhri, O. Prakash, J. Chem. Eng. Data **11**, 593 (1966)
55. M. Almasi, M. Shojabakhtiar, Thermochim. Acta **523**, 105 (2011)
56. J.A. González, I.G. de la Fuentá, J.C. Cobos, Fluid Phase Equilib. **168**, 31 (2000)
57. K.V. Zaitseva, M.A. Varfolomeev, V.B. Novikov, B.N. Solomonov, J. Chem. Thermodyn. **43**, 1083 (2011)
58. S. Verma, S. Gahlyan, M. Rani, S. Maken, Arab. J. Sci. Eng. **43**, 6087 (2018)
59. K. Kumari, S. Maken, J. Mol. Liq. **325**, 115170 (2021)